Proceedings 10th NUMGE 2023
10th European Conference on Numerical Methods in Geotechnical Engineering
Zdravkovic L, Kontoe S, Taborda DMG, Tsiampousi A (eds)

https://doi.org/10.53243/NUMGE2023-411

The significance of ground motion duration in assessing lateral displacement of liquefiable slopes

M. Asgarpoor[1], M. Taiebat[1]

[1]*Department of Civil Engineering, University of British Columbia, Vancouver, BC, Canada*

ABSTRACT: This paper presents a parametric study for assessing the lateral displacement of liquefiable slopes with a focus on comparing the outcomes for short- and long-duration motions. The study investigates the effects of increased loading cycles and shaking time in longer-duration motions, which alter the pre- and post-liquefaction responses of soil and impact the deformations of sloped sand deposits under seismic loading. The study models multi-layer soil columns with varying densities and thicknesses of the liquefiable layer using the SANISAND-MSf soil model in OpenSees. The models are subjected to a suite of spectrally equivalent short- and long-duration motions that are linearly scaled to a design spectrum based on a site in Vancouver with a 2% in 50 years hazard level. For the range of variables considered, the results show a direct linear correlation between lateral displacement and ground motion duration. Moreover, CAV_5 is found to be a more efficient intensity measure for predicting lateral deformations compared to $D_{5\text{-}95}$ and I_a. Additionally, based on an analysis of 60 ground motions, the study generally indicates that lateral displacements decrease with increasing in relative density and decreasing thickness of liquefiable soil.

Keywords: Liquefaction; Lateral spreading; Short- and long-duration ground motions; Nonlinear soil response.

1 INTRODUCTION

Lateral spreading refers to the development of surface displacements in saturated granular slopes due to cyclic liquefaction caused by seismic loading. Strength and stiffness loss, as a result of excess pore water pressure generation under cyclic loading, leads the saturated inclined deposits to experience large shear strains causing devastating deformations of slopes, dams, and bridges. Mechanics-based methodologies are required for estimating post-liquefaction deformations for performance-based and sustainable design of infrastructure systems. Numerous element-level tests and centrifuge experiments are available in the literature, which aid in validating and enhancing constitutive models of sand that are used in nonlinear dynamic analyses for the estimation of deformations caused by seismic excitation. Verification of Liquefaction Analyses and Centrifuge Studies (VELACS) (Arulanandan and Scott, 1993) was the pioneer set of physical modelling used to study liquefaction-induced deformations. The Canadian Liquefaction Experiment (CANLEX) (Robertson et al., 2000) was the subsequent step toward understanding the consequences of liquefaction in saturated sandy soils. The most recent step in this direction was the Liquefaction Experiments and Analysis Projects (LEAP) (Kutter et al., 2018, 2020), aimed at exploring the response of liquefiable sand deposits in the absence and presence of soil-structure interaction and under seismic excitation.

The available physical models consider only short-duration excitations, whereas, lateral spreading of liquefiable slopes can be affected by the duration of seismic ground motions. Although shallow, crustal earthquakes were commonly used to perform seismic analyses, there are vast areas in the world that are at risk of subduction earthquake motions (e.g., the Pacific Northwest). These ground motions have longer durations than crustal ground motions because of their higher magnitude and greater source-to-site distance. More loading cycles in longer-duration motions can intensify soil softening, leading to larger deformations of sloped sand deposits. Moreover, the increased shaking time may allow for the redistribution of excess pore water pressure, thereby changing the resulting post-liquefaction deformations.

Past numerical studies have investigated the effect of ground motion duration on different aspects of geotechnical engineering. Studies by Barbosa et al. (2014) concluded that longer-duration motions cause more damaging effects on the seismic response of soil-bridge systems due to more loading cycles. Greenfield (2017) explored the triggering and effects of liquefaction due to long-duration ground motions. Using nonlinear, effective stress analyses, some simulations with motions lasting long after the initial liquefaction showed dilation pulses, continued softening due to soil fabric degradation, and soil stiffening due to pore pressure dissipation and drainage. Khosravifar and Nasr (2017) studied the inelastic deformation of piles in the liquefiable sloped ground to assess how inertia and liquefaction-induced

lateral spreading combine in long- and short-duration motions.

The main objective of this paper is to explore the effect of ground motion duration on the lateral spreading of liquefiable slopes. For this purpose, a validated constitutive model was employed in a numerical multi-layer soil column model subjected to a variety of short- and long-duration motions scaled to 2% in a 50-year design spectrum in Vancouver. A parametric analysis is then conducted to assess the influence of changing ground motion duration on the lateral deformation of slopes with different soil densities and thicknesses.

2 SOIL CONSTITUTIVE MODEL

Performance-based assessment of liquefaction consequences requires a robust constitutive model of soil that is validated and calibrated using a range of element-level and centrifuge tests. The constitutive model used in this study is an improved version of the well-known stress-ratio controlled, critical state compatible, bounding surface plasticity model proposed by Dafalias and Manzari (2004), often referred to as DM04 model, which formed the basis of what was later named SANISAND class of models (Taiebat and Dafalias, 2008). The DM04 model considers a fabric-dilatancy internal variable that evolves in the dilative phase of shearing and enhances the shear-induced contraction in the subsequent reverse loading, hence allowing the reduction of mean effective stress p and simulating cyclic mobility type of liquefaction. Propagation of earthquake-induced shear waves through liquefied soils using the reference SANISAND model was investigated in the literature (Taiebat et al. 2010).

To address two major deficiencies of the DM04 model in simulating the undrained cyclic shearing, Yang et al. (2022) proposed the SANISAND-MSf (S-MSf) model, which has two constitutive ingredients: memory surface (M) and semifluidized state (Sf). The very fast development of pore pressure in pre-liquefaction under low cyclic stress ratios is controlled by the memory surface, which manages the rate of plastic deviatoric and volumetric strains evolution, and improves the number of cycles pre-liquefaction. The semifluidized state allows for the development and accumulation of large cyclic shear strains in the post-liquefaction by reducing the plastic shear stiffness and dilatancy while maintaining the same volumetric strain rate. This was achieved by a state internal variable named strain liquefaction factor by Barrero et al. (2020), which gets activated only in the state of very small effective stresses and allows the generation and accumulation of shear strains in post-liquefaction. The capabilities of the S-MSf model have been thoroughly validated against centrifuge tests of saturated liquefiable deposits prone to lateral spreading by Reyes et al. (2021), Perez et al. (2022), and Perez et al. (2023).

Table 1. SANISAND-MSf calibrated model parameters

Description	Symbol	Ottawa F65 sand
Elasticity	G_0	125
	υ	0.05
Critical state	M^c	1.26
	c	0.735
	e_c^{ref}	0.78
	λ_c	0.0287
	ξ	0.7
Yield surface	m	0.01
Kinematic hardening	n^b	4.0
	h_0'	4.0
	c_h	0.968
Dilatancy	n^d	2.5
	A_0'	0.626
	n_g	0.9
Fabric dilatancy	$z_{\max}$	15
	c_z	2000
Memory surface	μ_0	4.08
	u	3.23
Semifluidized state	x	5.0
	c_l	25

Cyclic torsional hollow-cylinder shear tests by Vargas et al. (2020) and more recent cyclic direct simple shear tests (CDSS) of Lbibb and Manzari (2023) are used for calibration and validation of Ottawa-F65 sand input parameters in this paper, as shown in Table 1. Liquefaction strength curves of Ottawa-F65 sand from CDSS tests at D_r=66% and σ_v' = 40kPa and with and without the static shear stresses ($\alpha = \tau_{\text{static}}/\sigma_v'$) are presented in Figure 1, comparing the experiments and simulations using the calibrated soil parameters of Table 1. The cyclic stress ratio (CSR) versus the number of cycles to reach 5% single amplitude shear strain resulted from simulations using S-MSf are in good agreement with experimental data.

3 NUMERICAL SIMULATIONS

The dynamic response of saturated soil columns is simulated in the finite element-based open-source program OpenSees (McKenna et al., 2000). The S-MSf model is implemented in OpenSees using a modified Euler method with an automatic sub-stepping error control integration scheme. Layered soil columns are numerically modelled with the aim of simulating infinite slopes. 20-

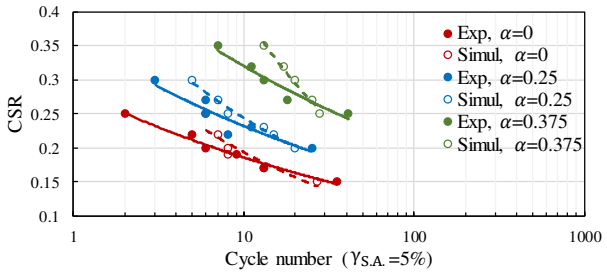

Figure 1. Liquefaction strength curves of Ottawa-F65 sand for CDSS tests with σ_v'=40 kPa and D_r=66%, with experimental data from Lbibb and Manzari (2023) and simulations using SANISAND-MSf

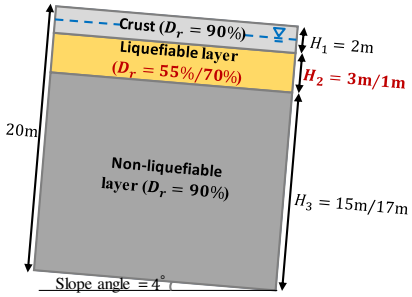

Figure 2: Schematic illustration of infinite slope

m vertical soil columns consisting of 40 eight-node brick elements (0.5 × 0.5 × 0.5m) are considered, including three layers: a non-liquefiable top layer with a constant thickness of 2m, a liquefiable mid-layer with the thickness of 3m or 1m, and bottom non-liquefiable layer with the thickness of 15m or 17m, as illustrated in Figure 2. A water table with a depth of 1m is assumed. SSPbrickUP elements consider coupled solid displacement-pore pressure (u-p) formulation, based on the work of Biot as extended by Zienkiewicz and Shiomi (1984). In these elements, the material response is recorded at the single integration point located in the centre of the element. The slope angle is considered by applying the horizontal gravity component in addition to the vertical gravity component. The out-of-plane deformations are constrained, and to simulate the 1D behavior, the lateral displacement of nodes is tied at each depth using 'equalDOF' command. To account for the finite rigidity of the underlying half-space, Lysmer-Kuhlemeyer's dashpot (1969) is defined using viscous uniaxial material, connected to the base node with a zero-length element. The velocity time history of seismic input motion is applied at the base of the soil column.

The models are constructed in two phases, starting with a nonlinear elastic S-MSf model and stabilizing under gravity loading to simulate hydrostatic pore water pressure, and initial effective stresses. In the second stage, the dynamic analysis is performed by subjecting the system to the input seismic shaking at its base. The isotropic fluid model with a water bulk modulus of 2.2 × 10^6 kPa and hydraulic conductivity of k = 0.0207×e_0-0.0009 (cm/s) is used as recommended by Kutter et al. (2020) for Ottawa-F65 sand, where e_0 is the initial void ratio of soil.

4 GROUND MOTION RECORDS

The duration of ground motions in this study is calculated based on the 5% to 95% significant duration (D_{5-95}), which is the time interval over 5% to 95% of the Arias Intensity. Thirty long-duration ground motions (combination of inslab and interface) with D_{5-95} > 30 s, as well as thirty short-duration ground motions with D_{5-95} < 30 s are selected from PEER NGA-Subduction and PEER NGA west2, respectively, considering factors such as magnitude, shear wave velocity, and source to

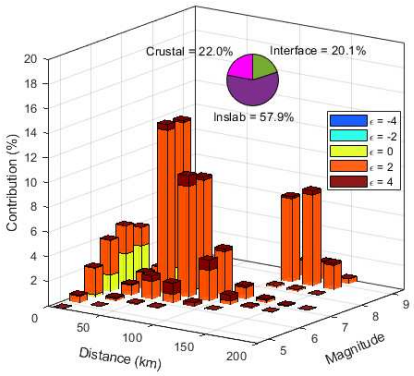

Figure 3. Seismic hazard disaggregation for Vancouver (City Hall) at 2% in 50 years hazard level (S_a (0.5s) = 0.77g)

site distance. To isolate the effect of duration from the effects of amplitude and response spectral shape, spectrally equivalent sets of short- and long-duration motions are selected using the method of Chandramohan et al. (2016).

The uniform seismic hazard spectra (UHS) of Vancouver (City Hall) with 2% in 50 years hazard level is specified as a design spectrum based on NBCC (2020). The short- and long-duration ground motions are linearly scaled to the design spectrum. A very dense deposit of site class C with shear wave velocity in the range of 360-760 m/s is considered for the base soil condition. Using the open-source software for seismic risk assessment OpenQuake (Silva et al. 2012), seismic hazard disaggregation of the site at a spectral acceleration of 0.77 g at the period of 0.5 s, which is the average natural period of the 20 m soil columns considered in this study, is shown in Figure 3. This figure shows the percentage of contribution of dominant seismic sources in the site, which is 78% from subduction earthquakes (58% from inslab and 20% from interface subduction), and 22% from crustal earthquakes. The response spectra of scaled long- and short-duration ground motions are compared with the UHS of Vancouver in Figure 4.

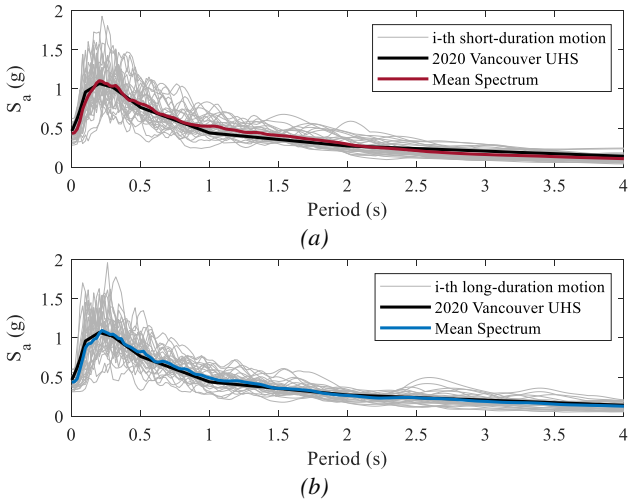

Figure 4. Comparison of response spectra of selected motions with the UHS of Vancouver: (a) short-duration motions and (b) long-duration motions

5 EFFECT OF GROUND MOTION DURATION

Multi-layer soil columns with non-liquefiable top and bottom layers and liquefiable mid-layer are considered in this study. Fabric dilatancy parameter c_z is assumed to be zero in the non-liquefiable layers, which deactivates the contraction after dilation phases upon loading reversal, and prevents the reduction of mean effective stresses close to zero. This is a necessary consideration to prevent taking the state to the semifluidized and associated large shear strains; hence very small lateral displacements are expected to happen in the non-liquefiable layers. The parabolic distribution of elastic shear modulus through depth can be adjusted by parameter G_0. Stiff soil with an average V_s of around 200 m/s is assumed for the non-liquefiable layers, whereas soft soil with an average V_s of around 110 m/s is considered for the mid-layer. Thus, the small strain shear modulus is adjusted by considering G_0 value to be 216 and 125 for non-liquefiable and liquefiable layers, respectively.

The spectral acceleration, acceleration time histories, and cumulative absolute velocity with 5 cm/s^2 threshold acceleration (CAV_5) of one pair of spectrally equivalent short- and long-duration motions (long-duration: Tokachi-oki, Japan, 2011, short-duration: Chuetsu-oki, Japan, 2007) are shown in Figure 5(a-c). Figure 5(c) suggests that the long-duration motion contains considerably larger energy than the short-duration motion. These motions are applied to the base of a soil column with H_2=3m and D_r=55% for the liquefiable layer, and the resulting surface lateral displacements (SLD) are compared in Figure 5(d). The large amplitudes of the applied motions make the soil liquefy relatively fast in both cases. However, given the larger energy of the long-duration motion, the resulting accumulation of shear strains during the post-liquefaction stage is higher compared to that for the case of short-duration motion. This is consistent with the observation of Perez et al. (2023) where they noted that the portion of CAV in the post-liquefaction stage appears to correlate with the resulting surface displacement.

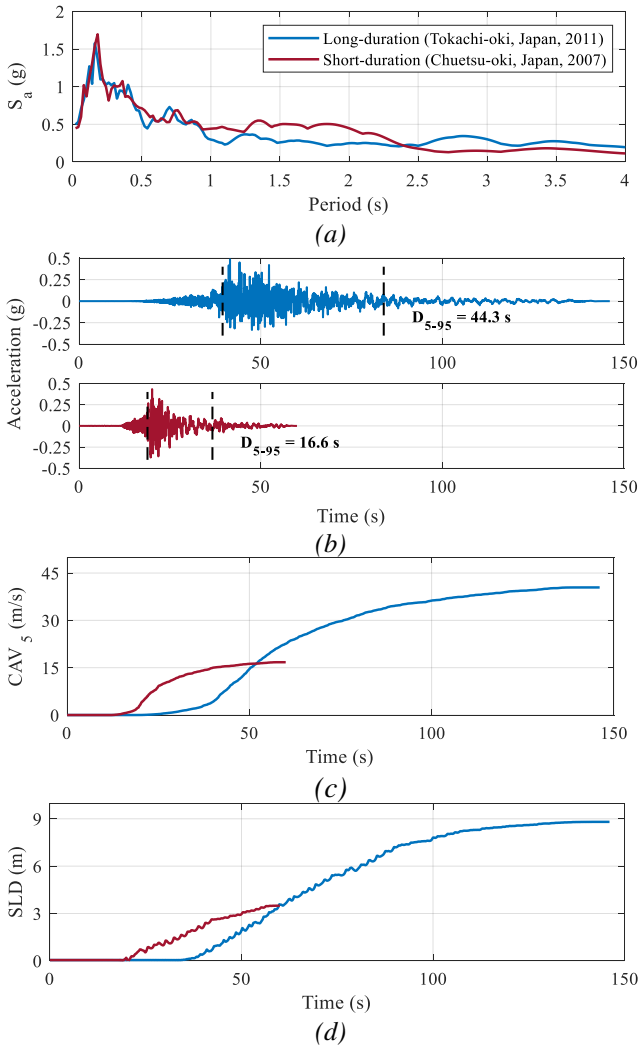

Figure 5. Comparison between (a) spectral acceleration, (b) acceleration time history, (c) CAV of spectrally equivalent long and short-duration motions records, and (d) the resulting surface lateral displacement, from the analysis of the soil column with H_2=3m and D_r=55%

6 PARAMETRIC STUDY

The lateral displacement of liquefiable slopes depends on various parameters, including the relative density and thickness of the soil layers. In this section, the sensitivity of the change in lateral displacements with the change of ground motion duration is investigated by considering different design variables. A total of 180 nonlinear dynamic analyses using 60 ground motions with $D_{5\text{-}95}$ of 4 to 120 s are carried out considering two design variables, including the relative density and thickness of the liquefiable layer. All soil columns have a slope angle of 4 degrees.

6.1 Relative density of liquefiable layer

Effects of the duration of ground motion on the surface lateral displacements (SLD) of the soil columns with H_2=3m and D_r=55% and 70% for the liquefiable layer are presented in Figure 6. The LD and SD in the legend of figures stand for long-duration and short-duration, respectively. Since all ground motions are chosen and scaled to a unique design spectrum to make their amplitude and response spectral shape close to each other, the differences between the obtained results are mostly attributed to the duration of motions. A direct correlation is observed between surface deformation and motion duration, which can be approximated by linear regression. The efficiency of the fitted equations is assessed by the coefficient of determination (R^2) and the root mean squared error as the standard error of estimation (σ_{est}). Surface displacements decrease as the relative

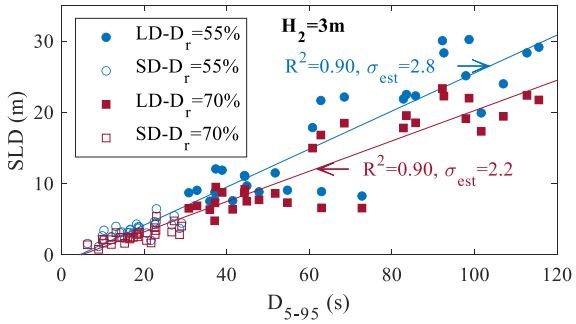

Figure 6. Effect of duration of ground motion on surface lateral displacements of the soil columns with different relative densities of the liquefiable layer

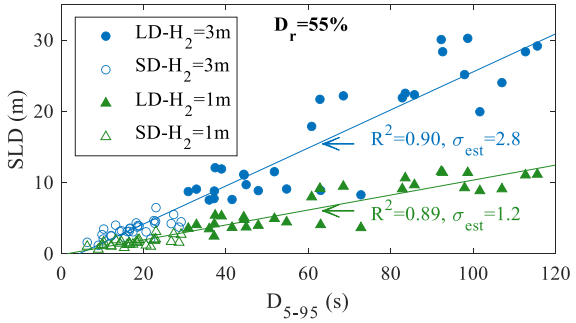

Figure 7. Effect of duration of ground motion on surface lateral displacements of the soil columns with different thicknesses of the liquefiable layer

density of the soil increases, which is consistent with experimental observations that soils with lower initial void ratios tend to have higher cyclic resistance.

6.2 *Thickness of liquefiable layer*

The change in the relationship between soil lateral displacement and base motion duration is investigated in Figure 7 by varying the thickness of the liquefiable layer from 3 to 1 m, and using the same relative density of 55%. The results show a decreasing displacement trend with decreasing thickness of the liquefiable layer, which is reasonable since a smaller portion of the soil is susceptible to liquefaction in the case of the thinner liquefiable layer.

6.3 *Efficient intensity measure*

The efficiency of cumulative absolute velocity (CAV_5) with 5 cm/s^2 threshold acceleration, and Arias intensity (I_a), as well as the significant duration in capturing the lateral displacement of liquefiable slopes, are evaluated in this section by assessing the values of R^2 and σ_{est} for the fitted line to the data. As shown in Figures 6-8, the higher R^2 and lower σ_{est} values of the fitted curves correspond to CAV_5 and $D_{5\text{-}95}$, respectively, reflecting their ability to correlate with lateral displacements.

Although all ground motions are scaled to the same design spectrum, they have different spectral shapes and intensities, the effect of which can be best captured by

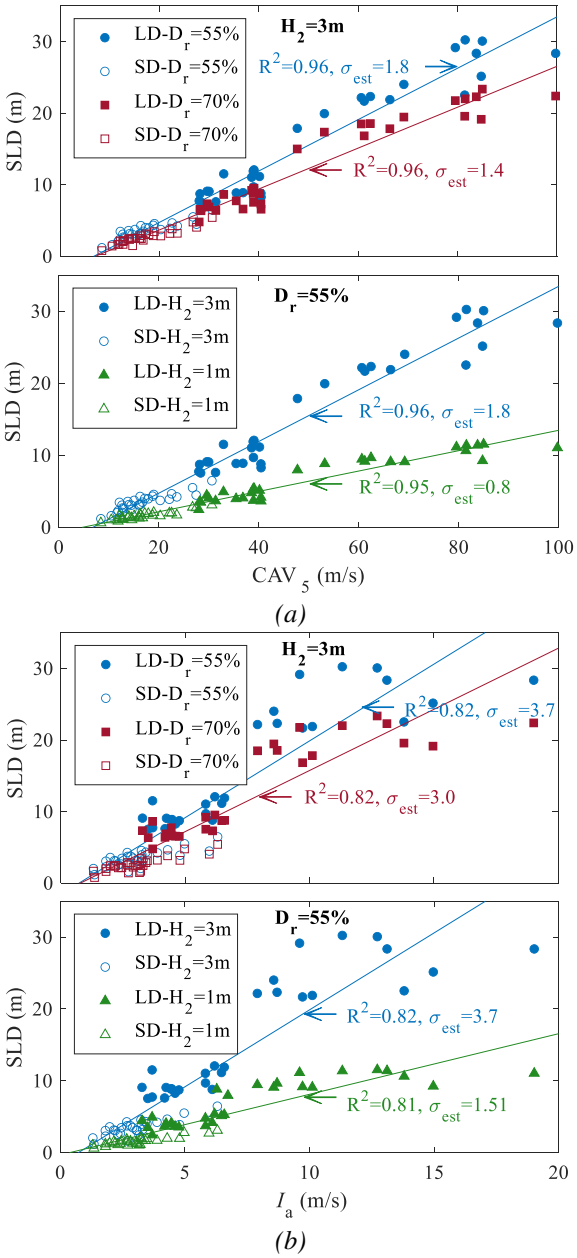

Figure 8. Efficiency evaluation of (a) CAV_5 and (b) I_a for prediction of surface lateral displacement of the soil columns with different relative densities and thicknesses of the liquefiable layer

CAV_5. The range of CAV_5 and I_a values shown in Figure 8 reveals the huge ground motion intensities that soil columns experienced during shaking, which resulted in large surface lateral displacements at the end of shaking. Moreover, the current semifluidized formulation, which is responsible for the post-liquefaction behaviour of the soil, tends to overestimate the shear strain development, causing large lateral displacements at the end of shaking when static shear stress presents. This overprediction gets amplified when soil stays longer in the liquefied state, as happens in longer-duration motions. The model deficiency in the presence of static shear stress is going to be addressed in the next studies.

7 CONCLUSIONS

This study presented a numerical modelling to evaluate the effect of ground motion duration on the lateral deformation of liquefiable infinite slopes. Three soil columns with different relative densities and thicknesses of the liquefiable layer were modelled in OpenSees using SANISAND-MSf model and were subjected to spectrally equivalent short- and long-duration motions. A direct correlation was observed between surface deformation and duration of motion, which was approximated by a linear regression with R^2 value higher than 0.9 and σ_{est} value of between 1.2m and 2.8m. Moreover, CAV_5 was found to have a better correlation with lateral deformation than $D_{5\text{-}95}$ and I_a. Analysing the models under all ground motions indicated the increase of lateral displacements with the decrease of relative density and increase of liquefiable layer thickness.

8 ACKNOWLEDGEMENTS

Financial support for this study was provided by the Natural Sciences and Engineering Research Council of Canada (NSERC).

9 REFERENCES

Arulanandan K., Scott RF., editors. 1993. Verification of numerical procedures for the analysis of soil liquefaction problems. *Proceedings of the International Conference on the Verification of Numerical Procedures for the Analysis of Soil Liquefaction Problems*, Balkema.

Barbosa, A.R., Mason, H.B., Romney, K. 2014. SSI-Bridge: Soil Bridge Interaction During Long-Duration Earthquake Motions (No. 2012-S-OSU-0008), *Pacific Northwest Transportation Consortium*.

Barrero, A.R., Taiebat, M., Dafalias, Y.F. 2020. Modeling cyclic shearing of sands in the semifluidized state. *International Journal for Numerical and Analytical Methods in Geomechanics* **44**, 371-388.

Chandramohan R, Baker J.W., Deierlein G.G. 2016. Quantifying the influence of ground motion duration on structural collapse capacity using spectrally equivalent records. *Earthquake Spectra* **32**, 927–50.

Dafalias Y.F., Manzari M.T. 2004. Simple plasticity sand model accounting for fabric change effects. *Journal of Engineering mechanics* **130**, 622–34.

Greenfield, M.W. 2017. Effects of long-duration ground motions on liquefaction hazards. Ph.D. Dissertation, University of Washington, Seattle, WA.

Khosravifar, A., Nasr, J. 2017. Modified design procedures for bridge pile foundations subjected to liquefaction-induced lateral spreading. *DFI Journal-The Journal of the Deep Foundations Institute*, **11**(2-3), 114-127.

Kutter, B.L., Carey T.J., Hashimoto, T., Zeghal, M., et al. 2018. LEAP-GWU-2015 experiment specifications, results, and comparisons. *Soil Dynamics and Earthquake Engineering* **113**, 616–28.

Kutter, B.L., Manzari, M.T., Zeghal, M. 2020. *Model Tests and Numerical Simulations of Liquefaction and Lateral Spreading LEAP-UCD-2017*. Springer, Switzerland.

Lbibb, S., Manzari, M.T. 2023. Stress-strain behavior of Ottawa sand in cyclic direct simple shear and modelling of cyclic strength using Artificial Neural Networks. *Soil Dynamics and Earthquake Engineering* **164**, 107585.

Lysmer, J., Kuhlemeyer, A.M. 1969. Finite dynamic model for infinite media, *Journal of the Engineering Mechanics Division*, ASCE **95**, 859-877.

McKenna F, Fenves G.L., Scott M.H., Jeremic B. 2000. Open System for Earthquake Engineering Simulation (OpenSees). *Pacific Earthquake Engineering Research Center,* Berkeley (CA), University of California.

NBCC. National building code of Canada, 15th Edition, 2020. Canadian commission on building and fire codes. Ottawa, Ontario, Canada: National Research Council of Canada.

Perez, K., Reyes, A., Taiebat, M. 2022. Numerical modelling of the LEAP-RPI-2020 centrifuge tests using SANISAND-MSf. *Performance-based Design in Earthquake. Geotechnical Engineering (PBD-IV)*, 15-19 July, Beijing, China.

Perez, K., Reyes, A., and Taiebat, M. 2023. Roles of pre- and post-liquefaction stages in dynamic system response of liquefiable sand retained by a sheet-pile wall. *Soil Dynamics and Earthquake Engineering* **171**, 107937.

Reyes, A., Yang, M., Barrero, A.R., Taiebat, M. 2021. Numerical modeling of soil liquefaction and lateral spreading using the SANISAND-Sf model in the LEAP experiments. *Soil Dynamics and Earthquake Engineering* **143**, 106613.

Robertson, P.K., et al. 2000. The CANLEX project: summary and conclusions. *Canadian Geotechnical Journal* **37**(3), 563-591.

Silva, V., Crowley, H., Pagani, M., Monelli, D., Pinho, R. 2012. Development and application of OpenQuake, an opensource software for seismic risk assessment, *Proceedings of the 15th World Conference on Earthquake Engineering*, Lisbon, Portugal, 4917.

Taiebat, M., Dafalias, Y.F. 2008. SANISAND: simple anisotropic sand plasticity model. *International Journal of Numerical and Analytical Methods in Geomechanics* **32(8)**, 915–48.

Taiebat, M., Jeremić, B., Dafalias, Y.F., Kanya, A.M., Cheng, Z. 2010. Propagation of seismic waves through liquified soils. *Soil Dynamics and Earthquake Engineering* **30(4)**, 236–257.

Vargas, R.R., Ueda, K., Uemura, K. 2020. Influence of the relative density and K0 effects in the cyclic response of Ottawa F-65 sand-cyclic Torsional Hollow-Cylinder shear tests for LEAP-ASIA-2019. *Soil Dynamics and Earthquake Engineering* **133**, 106111.

Yang, M., Taiebat, M., Dafalias, Y.F. 2022. SANISAND-MSf: a sand plasticity model with memory surface and semifluidised state. *Géotechnique* **72**, 227-246.

Zienkiewicz, O.C., Shiomi, T. 1984. Dynamic behaviour of saturated porous media; the generalized Biot formulation and its numerical solution. *International journal for numerical and analytical methods in geomechanics* **8(1)**, 71-96.